Development of astroglia heterogeneously expressing Pax2, vimentin and GFAP during the ontogeny of the optic pathway of the lizard (Gallotia galloti): An immunohistochemical and ul…

Article *in* Cell and Tissue Research · August 2011

DOI: 10.1007/s00441-011-1211-9 · Source: PubMed

CITATIONS
11

READS
145

7 authors, including:

Elena Santos
Universidad de La Laguna
17 PUBLICATIONS **107** CITATIONS
SEE PROFILE

Carmen M Yanes
Universidad de La Laguna
55 PUBLICATIONS **717** CITATIONS
SEE PROFILE

Maria del Mar Romero-Alemán
Universidad de Las Palmas de Gran Canaria
37 PUBLICATIONS **240** CITATIONS
SEE PROFILE

Carmen Alfayate
Universidad de La Laguna
28 PUBLICATIONS **109** CITATIONS
SEE PROFILE

Cell Tissue Res
DOI 10.1007/s00441-011-1211-9

REGULAR ARTICLE

Development of astroglia heterogeneously expressing Pax2, vimentin and GFAP during the ontogeny of the optic pathway of the lizard (*Gallotia galloti*): an immunohistochemical and ultrastructural study

M. Nieves Casañas · Elena Santos · Carmen Yanes · Maria M. Romero-Alemán · Raquel Viñoly · M. Carmen Alfayate · Maximina Monzón-Mayor

Received: 15 February 2011 / Accepted: 13 July 2011

Abstract The successful regrowth of retinal ganglion cell (RGC) axons after optic nerve (ON) axotomy in *Gallotia galloti* indicates a permissive role of the glial environment. We have characterised the astroglial lineage of the lizard optic pathway throughout its ontogeny (embryonic stage 30 [E30] to adults) by using electron microscopy and immunohistochemistry to detect the proliferation marker PCNA (proliferating cell nuclear antigen), the transcription factor Pax2 and the gliofilament proteins vimentin (Vim) and GFAP (glial fibrillary acidic protein). $PCNA^+$ cells were abundant until E39, with $GFAP^+/PCNA^+$ astrocytes being observed between E37 and hatching. Proliferation diminished markedly afterwards, being undetectable in the adult optic pathway. Müller glia of the central retina expressed Pax2 from E37 and their endfeet accumulated Vim from E33 and GFAP from E37 onwards. Astrocytes were absent in the avascular lizard retina, whereas abundant $Pax2^+$ astrocytes were observed in the ON from E30. A major subpopulation of these astrocytes coexpressed Vim from E35 and also GFAP from E37 onwards; thus the majority of mature astrocytes coexpressed Pax2/Vim/GFAP. The astrocytes were ultrastructurally identified by their gliofilaments, microtubules, dense bodies, desmosomes and glycogen granules, which preferentially accumulated in cell processes. Astrocytes in the adult ON coexpressed both gliofilaments and presented desmosomes indicating a reinforcement of the ON structure; this is physiologically necessary for local adaptation to mechanical forces linked to eye movement. We suggest that astrocytes forming this structural scaffold facilitate the regrowth of RGCs after ON transection.

Keywords Astrocytes · Visual system · Development · Ultrastructure · Reptiles · *Gallotia galloti (Lacertilia)*

Abbreviations

CN	Caudal optic nerve
CPONJ	Conus papillaris-optic nerve junction
CR	Central retina
GFAP	Glial fibrillary acidic protein
INL	Inner nuclear layer
MN	Mid optic nerve
OCh	Optic chiasm
ON	Optic nerve

Electronic supplementary material The online version of this article (doi:10.1007/s00441-011-1211-9) contains supplementary material, which is available to authorized users.

This work was supported by the Spanish Ministry of Education (Research Project BFU2007-67139) and the Regional Canary Islands Government (ACIISI, Research Project SolSubC200801000281; Project ULPAPD-08/01-4).

M. N. Casañas · E. Santos · C. Yanes · R. Viñoly · M. C. Alfayate
Department of Cellular Biology, Faculty of Biology,
University of La Laguna,
38206 Tenerife, Canary Islands, Spain

E. Santos (✉) · M. M. Romero-Alemán · M. Monzón-Mayor
Department of Morphology (Cellular Biology),
Faculty of Health Sciences,
University of Las Palmas of Gran Canaria,
C/ Dr. Pasteur s/n. A.C. 550,
35016 Las Palmas, Canary Islands, Spain
e-mail: esantos@proyinves.ulpgc.es

Published online: 09 August 2011

ONH	Optic nerve head
OTr	Optic tract
PCNA	Proliferating cell nuclear antigen
PR	Peripheral retina
RGC	Retinal ganglion cell
RONJ	Retina-optic nerve junction
Vim	Vimentin

Introduction

Only two reptilian species, including *Gallotia galloti*, have shown the spontaneous regrowth of retinal ganglion cell (RGC) axons as far as the tectum after optic nerve (ON) axotomy (Dunlop et al. 2004; Lang et al. 1998). Unlike in mammals, the persistent astroglial scar, which, in lizard, expresses glial fibrillary acidic protein (GFAP; Lang et al. 2002, 2008) and neurotrophin-3 (NT-3; Santos et al. 2008), is permissive to axon regrowth. The astroglial lineage of the optic tectum of *G. galloti* has been studied in detail during ontogeny (Monzón-Mayor et al. 1990a, b, c, 1998; Romero-Alemán et al. 2003), whereas in the rest of the optic pathway, these cells are still poorly characterised (Alfayate et al. 2011; Romero-Alemán et al. 2003, 2010). We consider that the further characterisation of the astroglial lineage during development would be helpful for understanding RGC axon growth and regrowth, since both might require similar astroglial environments. In the vertebrate retina, Müller glia represent the main astroglial type providing structural support to the delicate retinal tissue. In avascular retinae lacking astrocytes (i.e. chick), Müller glia are considered to replace most of their functions (Won et al. 2000).

In general, astrocytes share common ultrastructural features in all vertebrates: intermediate filaments, glycogen granules and euchromatic nuclei (Maggs and Scholes 1990) and dense bodies related to developmental degeneration events (Wolburg and Bäuerle 1993). Unique to fish and amphibians, but uncertain in reptiles, ON astrocytes express cytokeratin filaments and are connected by intercellular desmosomes as reinforcement (Maggs and Scholes 1990; Rungger-Brändle et al. 1989), whereas GFAP is restricted to the glia limitans of the optic nerve head (ONH) and to optic tract (OTr) astrocytes (Levine 1989). In birds and mammals, ON astrocytes contain neither cytokeratin nor desmosomes, but rather vimentin (Vim) and high levels of GFAP (see Discussion). Gliofilaments are involved in the maintenance of cellular shape, resistance to mechanical stress, cell mobility (Lepekhin et al. 2001) and cytoplasmic trafficking of exocytic vesicles (Kreft et al. 2009; Potokar et al. 2007). Moreover, astrocytes are specialised in the maintenance of ionic and metabolic homeostasis, axon guidance (Bixby and Harris 1991; Brodkey et al. 1993), blood-brain barrier formation (Rubin and Staddon 1999) and the modulation of neuronal activity (Kimelberg 2010; Pereira and Furlan 2010).

Our previous studies in the developing and adult lizard midbrain have revealed that Vim and GFAP are restricted to astrocytes, whereas S100 and glutamine synthetase identify a subpopulation of oligodendrocytes (Monzón-Mayor et al. 1998; Romero-Alemán et al. 2003). Therefore, we have focused, in this study, on the expression of Pax2 and the gliofilaments Vim and GFAP, since they are highly conserved in vertebrates and allow a comparison with other regeneration-competent (i.e. fish, amphibians) and regeneration-deficient (i.e. chicken, mammals) species. Pax2 is a transcription factor involved in differentiation towards the astroglial lineage in the retina and ON by inhibiting neurogenesis (Boije et al. 2010; Chu et al. 2001; Stanke et al. 2010) and its expression along the optic stalk and ventral diencephalon is pivotal to axonal guidance, fasciculation and chiasm development (Alvarez-Bolado et al. 1997; Macdonald et al. 1997; Parrilla et al. 2009; Torres et al. 1996). In amniotes, one of the first events in the differentiation of the astroglial lineage is the expression of Vim. A shift from Vim to GFAP is followed by the eventual predominance of GFAP in mature astrocytes (Bodega et al. 1995; Dahl et al. 1981; Monzón-Mayor et al. 1990a).

We have studied cell proliferation by means of proliferating cell nuclear antigen (PCNA) in the developing lizard retina-OTr to complement the immunohistochemical characterisation of differentiating astrocytes and to check whether proliferation persists in the retina of adult *G. galloti*. In fish and amphibians, proliferating stem cells in the adult marginal retina are the basis for their continuous eye growth and functional regeneration ability (for a review, see Mitashov 2001).

In the vertebrate ON, several authors have reported intra- and interspecific heterogeneous populations of astroglial cells with regard to the expression of markers (see Discussion), spatial arrangement and ultrastructural features linked to functional specialisation and various degrees of maturation (Raff 1989; Scholes 1991; Stensaas 1977; Ye and Hernández 1995). Thus, the glia limitans of the vertebrate ONH typically consists of fibrous astrocytes at the vitreal region and peculiar astrocytes-Müller cells at the retina-optic nerve junction (RONJ; Dávila et al. 1987; Hirata et al. 1991; Lillo et al. 2002; Prada et al. 1989; Quesada et al. 2004; Triviño et al. 1996). In the proper ONH, astrocytes are arranged in columns that become more evident and numerous at the level of the sclera (Dávila et al. 1987; Gerhardt et al. 1999; Lillo et al. 2002; Morcos and Chan-Ling 2000; Oyama et al. 2006; Triviño et al. 1996; Ye and Hernández 1995). In the mammalian extraocular ON, astrocytes are classified into type-1 (fibrous), which give

rise to the limiting membranes and are in intimate contact with blood vessels, whereas type-2 are associated with Ranvier nodes (Miller et al. 1989a, b; Raff 1989). However, this classification excludes scarce astrocytes with intermediate characteristics (Suárez and Raff 1989). In the vertebrate OTr, astrocytes are less numerous, as radial glia spanning from the third ventricle are predominant (Levine 1989; Onteniente et al. 1983). By correlating these data with those of the present study, we hope to gain insights into the histophysiology and plasticity that support axon growth/regrowth under developing and regenerating conditions.

Materials and methods

Animals, tissue fixation and embedding

We used a total of 24 embryos from embryonic stage 30 [E30] to hatching, 10 postnatals (2–4 months) and 12 adults of *G. galloti*, a lizard indigenous to the Canary Islands. Fertilised eggs and adult animals were collected in the wild under licence and were maintained and treated in the laboratory according to Spanish and European animal welfare legislation. The stages of embryonic development were defined according to the tables of *G. galloti* (Ramos-Steffens 1980) and *Lacerta vivipara* (Dufaure and Hubert 1961). Postnatal and adult lizards were kept in large holding tanks fitted with heaters and overhead lighting (daily cycles of 12 h light/dark) and were allowed free access to water and to a mixed diet of fresh fruit and commercially available cat food. The temperature in the holding tanks was maintained around 20°C according to the average temperature in their natural environment. Adult lizards were anaesthetised by intraperitoneal injection with Diazepam (0.2 mg/kg)+ketamine (60 mg/kg) before transcardial perfusion (Bouin´s fixative or paraformaldehyde), whereas embryos and postnatals were anaesthetised with 15 mg/kg sodium pentothal and their brains were dissected and immersed in the same fixatives for 6 h. Paraformaldehyde-fixed brains were then cryoprotected in 30% sucrose in phosphate-buffered saline (PBS) overnight, embedded in Tissue-tek, frozen at −80°C and finally cut at 14 μm in the horizontal plane in a Reichert-Jung cryostat. Bouin-fixed brains were embedded in paraffin and cut at 10 μm in the horizontal plane on a Reichert-Jung microtome.

Antibody characterisation

The rabbit polyclonal anti-GFAP antibody (Biotrend, Germany; catalogue no. K39) and the mouse monoclonal anti-GFAP antibody (Sigma, USA; catalogue no. G3893) were raised against GFAP preparations from human and pig spinal cord, respectively, and recognise a single protein band of 51-55 kDa in Western blots of a wide variety of vertebrates. These antibodies gave identical staining pattern in the lizard brain to those reported previously (Monzón-Mayor et al. 1990a; Romero-Alemán et al. 2003, 2004, 2010).

The mouse monoclonal anti-Vim antibody (DSHB, USA; catalogue no. H5) raised against chicken optic tectum gave a staining pattern equivalent to that described in *G. galloti* by Yanes et al. (1990), i.e. stained astrocytes.

The rabbit polyclonal anti-Pax2 antibody (Covance, USA) was raised against human Pax2 protein (amino acids 188–385) and recognises Pax2a and Pax2b isoforms in a 44-kDa protein band on Western blots (manufacturer's datasheet). The Pax2 antibody produced a staining pattern in the lizard ON that was consistent with previous studies in fish (Parrilla et al. 2009), in chick and mammals (Stanke et al. 2010) and in lizard (Romero-Alemán et al. 2010).

Finally, the mouse monoclonal anti-PCNA (Novocastra, Sigma) recognises a 36-kDa protein and reacts in all vertebrate species and insects (manufacturer´s datasheet). Additionally, it has been previously used by Romero-Alemán et al. (2004) to monitor proliferation in lizard brain.

Western blot analyses

Brains of adult lizards were homogenised in ice-cold lysis buffer (20 mM TRIS-HCl pH 8, 137 mM NaCl, 10% glycerol, 1% Triton X-100) containing a protease inhibitor cocktail (Complete, Roche, Nutley, N.J., USA). Homogenates were centrifuged at 13,000*g* for 15 min at 4°C. The supernatants containing tissue extracts were collected and the protein concentration was measured according to the method of Bradford. Tissue extracts and molecular weight markers (Colorburst, Sigma) were subjected to electrophoresis on 10% sodium dodecyl sulfate polyacrylamide gels. Separated proteins were electroblotted onto nitrocellulose membranes (Hybond ECL, Amersham, Arlington Heights, Ill. USA). Membranes were blocked for 2 h in TBS (20 mM TRIS-HCl, 150 mM NaCl, pH 7) containing 5% skimmed milk and then incubated overnight with the mouse monoclonal primary antibodies (anti-GFAP, anti-Vim or anti-PCNA) described above. Following incubation with the appropriate anti-mouse horseradish-peroxidase-conjugated secondary antibody (1/20,000; SantaCruz Biotechnology, USA.), immunoreactive bands were visualised by enhanced chemiluminescence detection (Pierce, Rockford, Ill., USA) according to the manufacturer's instructions. Negative controls consisted of omission of the primary antibodies or use of the purified mouse IgG from pooled mouse normal serum (Sigma) instead of the corresponding primary antibodies.

Immunohistochemistry

We performed single immunoperoxidase labelling for the detection of PCNA, Vim or GFAP with mouse monoclonal antibodies. Sections were first preincubated in TBS (0.05 M Trizma base containing 150 mM NaCl, pH 7.4) containing 1% bovine serum albumin (BSA) for 24 h at 4°C to block non-specific staining and then permeabilised in a solution of 0.5% Triton X-100 in TBS for 10 min. The endogenous peroxidase was blocked in a solution of 3% H_2O_2 in TBS. For PCNA, we performed antigen retrieval before incubation in the primary antibody. Sections were incubated in the primary antibodies diluted in TBS with 0.2% Triton X-100 and 1% BSA, at room temperature (dilutions: anti-Vim 1:20, anti-GFAP 1:200, anti-PCNA 1:60). After being washed 3 times for 10 min in TBS, sections were incubated in the appropriate biotinylated secondary antibodies (Vector, 1:200) for 1 h followed by Avidin-peroxidase (Sigma,1:400) for 1 h and any immunostaining was revealed with diaminobenzidine. Double-immunoperoxidase labelling for the detection of PCNA and GFAP was performed by using sequential detection of the antigens. Sections were first incubated in the monoclonal anti-PCNA, revealing this antibody in brown as described above. Subsequently, sections were incubated in the monoclonal anti-GFAP and revealed in blue with 4-chloro-naphthol.

Single- and double-immunofluorescence stainings were performed for the single or simultaneous detection of Pax2 (polyclonal anti-rabbit, 1:200) and GFAP or Vim (monoclonals). Secondary antibodies were anti-rabbit Cy3 (Jackson; 1:1000) and anti-mouse Alexa Fluo 488 (Molecular Probes; 1:1000), incubated for 1 h at room temperature.

Negative controls consisted of either omitting the primary antibodies or using the purified mouse or rabbit IgG from pooled mouse or rabbit normal serum (Sigma), instead of the corresponding primary antibodies. All these negative controls resulted in the absence of immunostaining.

Electron microscopy

Three adults, 3 postnatals and 12 embryos at various developmental stages (E34, E35, E37, E39, E40, and hatching) were anaesthetised as previously reported. Adults were perfused transcardially by using 2.5% glutaraldehyde in 0.1 M Milloning buffer, pH whereas postnatals and embryos were decapitated. The retinas, ONs and optic chiasm-optic tracts were dissected and postfixed in the same fixative for 4 h at 4ºC. After being washed in Milloning buffer, the tissue samples were immersed in 1% osmium tetroxide for 4 h at room temperature and then dehydrated in graded acetone. The tissue samples were stained with 2% uranyl acetate in 70% ethanol overnight during the dehydration procedure and finally embedded in Araldite. Semithin sections (1 μm thick) and ultrathin sections (80 nm thick) were stained with toluidine blue and lead citrate, respectively.

Image acquisition and processing

Photomicrographs were taken via a Leica DM4000 B and a Zeiss Axiovert 200 M light microscope equipped with epifluorescence and a Leica DFC300 FX camera and an Axiocam HRm camera, respectively. Ultrathin sections were observed and captured via a Jeol 1010 (ULL) or a Zeiss 910 (ULPGC) electron microscope. Images were digitally processed by using Adobe Photoshop CS software. Only general contrast and brightness adjustments were made and figures were not otherwise manipulated.

Results

The lizard visual system is depicted in Fig. 1a, b. In Western blots, each antibody used in the current study recognised a single protein band in the brain samples of *G. galloti* (Fig. 1c) in accordance with the predicted molecular weight of the relevant antigens in other species. This indicated an interspecies conservation of the corresponding epitopes. All the negative controls were unlabelled, thus supporting the veracity of the following immunohistochemical results.

Immunohistochemical and ultrastructural characterisation of Müller glia during ontogeny of lizard retina

By E33, the lizard retina consisted of a pseudostratified neuroepithelium with a primitive nerve fibre layer and inner plexiform layer in the more differentiated central retina (CR). Vitreal endfeet expressed Vim from E33 onwards (Fig. 2a). Accordingly, electron-microscopy observations at E34-E35 revealed developing endfeet rich in gliofilaments and developed endoplasmic reticulum (not shown). Moreover, the basal lamina forming the inner limiting membrane was evident. During ontogeny, Vim staining was more intense in the peripheral retina (PR; Fig. 2b) than in the CR (Fig. 2c; see also Electronic Supplementary Material, Fig. S1a). In adult lizards, Vim was additionally detected in secondary Müller glia processes at the inner plexiform layer, mainly at the PR, and in the non-pigmentary epithelium of the ciliary body (Fig. 2h). $PCNA^+$ nuclei were abundantly observed in the retinal nuclear layers by E35 (Fig. 2d). By E37, they decreased in the CR (Fig. 2e) but not in the marginal retina and non-pigmented epitheli-

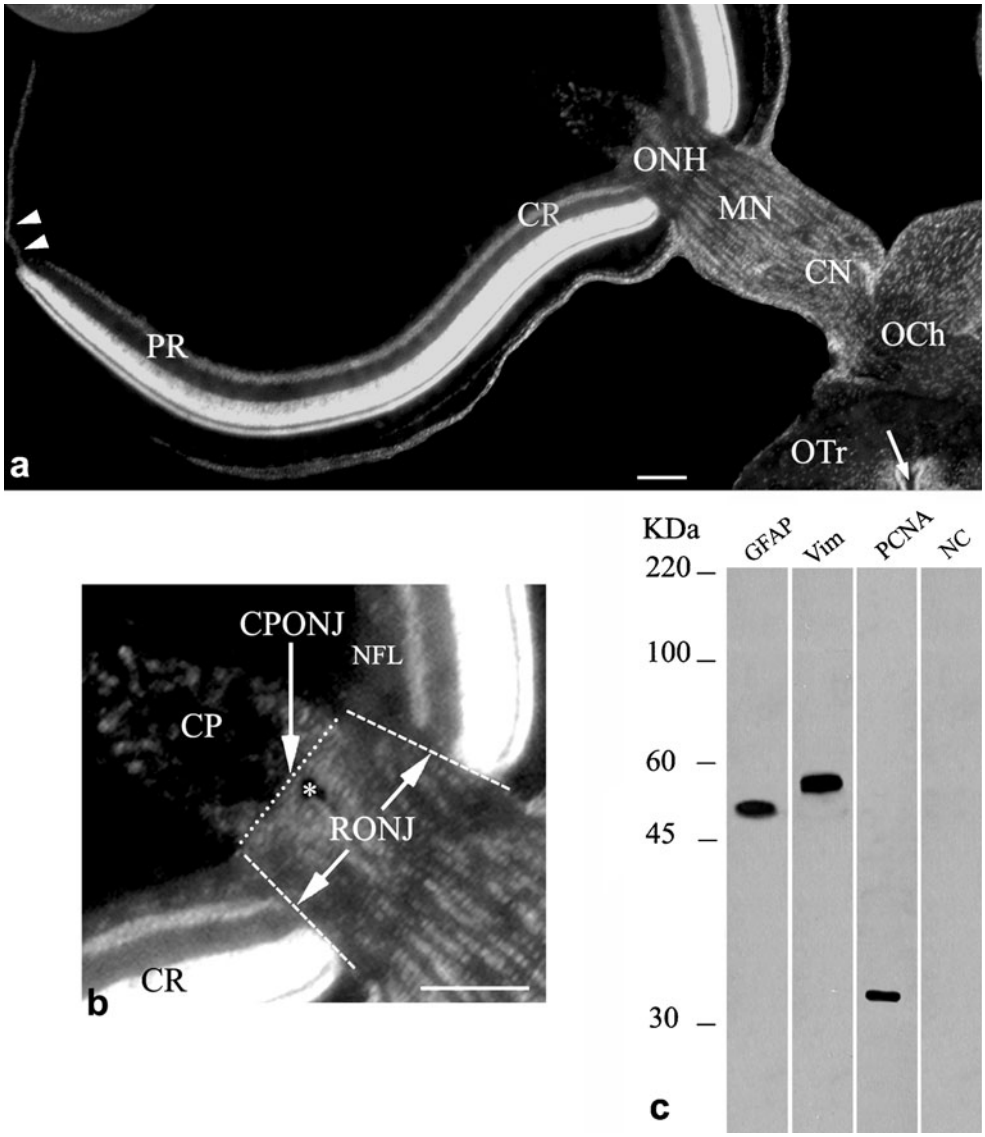

Fig. 1 **a** Dapi^{+} (4,6-diamidino-2-phenylindole) panoramic view of a horizontal section of the lizard visual pathway at embryonic stage 39 (E39). The central retina (*CR*) is located around the optic nerve head (*ONH*). The peripheral retina (*PR*) is much thinner at its far edge, which extends into the non-pigmented epithelium of the ciliary body (*arrowheads*). Note the location of the mid optic nerve (*MN*), caudal optic nerve (*CN*), optic chiasm (*OCh*) and optic tract (*OTr*) next to the hypothalamic ventricle (*arrow*). **b** Details of the ONH (asterisk central ophthalmic vessels), conus papillaris (*CP*) and CR. Note that the ONH is attached to the retina by the retina-optic nerve junction (*RONJ*) and to the CP by the conus papillaris-optic nerve junction (*CPONJ*). *Bars* 100 μm. **c** Western blot analysis of brain extracts of *G. galloti*. Note that each antibody (mouse monoclonal) recognises a single protein band of an apparent molecular weight similar to that described in other species: glial fibrillary acidic protein (*GFAP*; 51 kDa), vimentin (*Vim*; 57 kDa) and proliferating cell nuclear antigen (*PCNA*; 35 kDa). No signals are detectable in negative controls (*NC*). The apparent molecular weights (in kDa) of the marker proteins are shown *left*. This analysis is representative of three different animals

um of the ciliary body in which intense proliferation persisted (Fig. 2f). Proliferating cells were undetectable in postnatal and adult animals (Fig. 2g, h). From E37 to the adult stage, endfeet of the entire retina also expressed GFAP (Fig. 2i; see Electronic Supplementary Material, Fig. S1b). However, Pax2^{+} nuclei were detected only in the inner nuclear layer (INL) of the CR (Fig. 2j). Their elongated appearance and their location within the middle of the INL strongly suggested that they corresponded to Müller glia. Moreover, Pax2^{+} elongated glial nuclei were aligned and clustered in the RONJ (Fig. 2j). Müller glia was apparently the only astroglia residing in the lizard avascular retina as suggested by the absence of other glial types expressing Pax2, Vim or GFAP during the ontogeny.

Müller glia showed dense bodies and medium electron density in embryos (Fig. 2k, l) but exhibited markedly

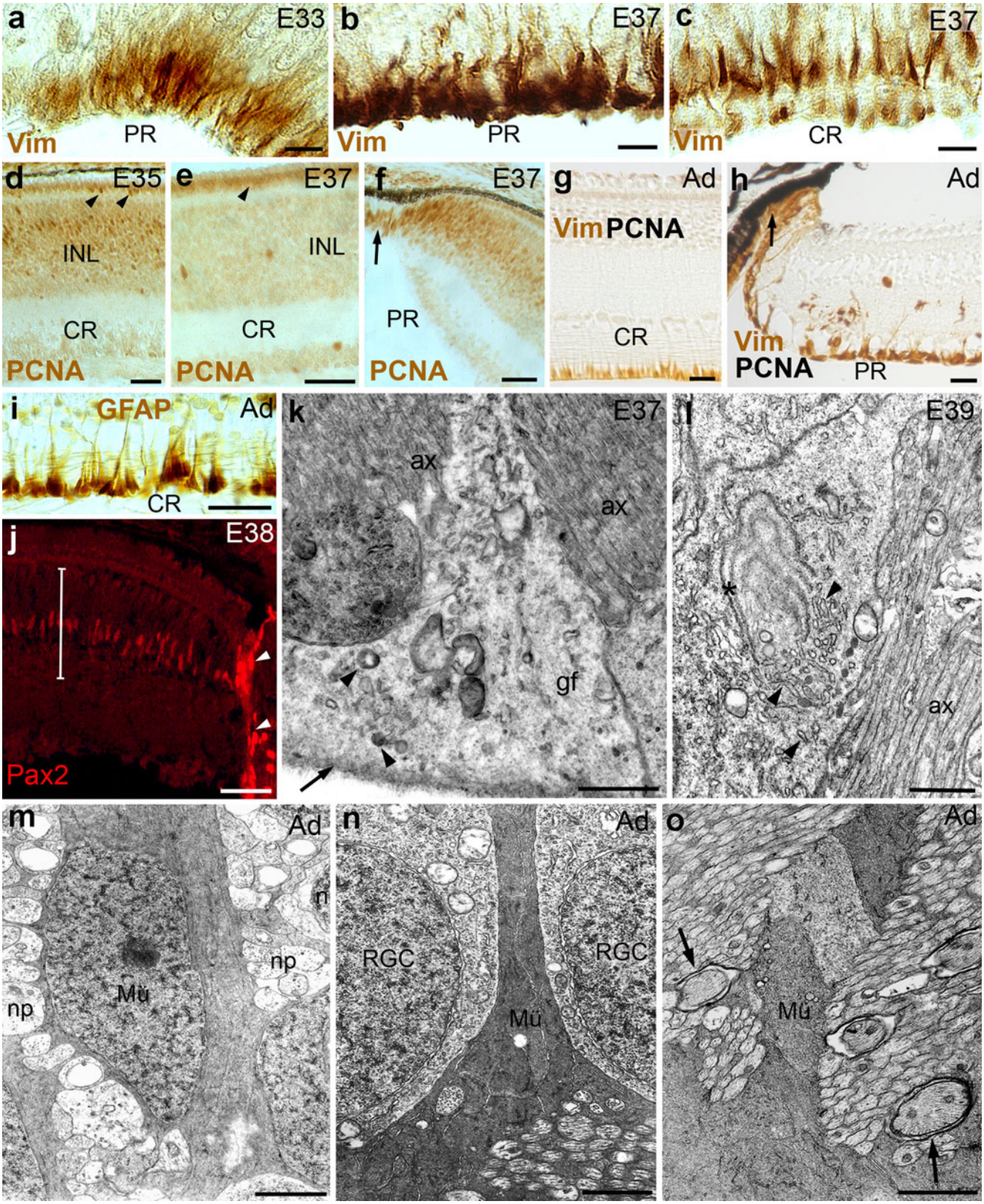

electron-dense cell bodies (Fig. 2m) and processes (Fig. 2n, o) in adults; these processes covered the ganglion cells and often contacted loosely myelinated axons. Sparse microtubules and abundant gliofilaments were observed in their vitreal processes along the ganglion cell layer (Fig. 2n) and nerve fibre layer (Fig. 2o).

◀ **Fig. 2** Immunostaining for vimentin (*Vim*), Pax2, glial fibrillary acidic protein (*GFAP*) and proliferating cell nuclear antigen (*PCNA*) in the retina and ultrastructure of Müller glia during ontogeny of lizard retina. **a–c** Immunoperoxidase staining for Vim in Müller glia endfeet. Peripheral retina (*PR*) at E33 (**a**). Peripheral (**b**) and central retina (**c**) at E37 within the same tissue section. Note the strongest labelling in the PR. **d–f** PCNA staining shows abundant proliferating cells in the inner (*INL*) and outer nuclear layers (*arrowheads*) of the central retina (*CR*) at E35 (**d**), whereas scarce proliferating cells are detected at E37 (**e**). The retinal margin and the non-pigmented epithelium of the ciliary body (*arrow*) contain a cluster of proliferating cells at E37 (**f**). **g–h** Double-staining for Vim/PCNA in the adult (*Ad*) retina shows the absence of proliferating cells in the CR (**g**), retinal margin (**h**) and non-pigmented epithelium of the ciliary body (*arrow* in **h**). Müller glia accumulate Vim in their vitreal endfeet, with stronger staining in the PR compared with the CR. Additionally, short Müller glia processes within the inner plexiform layer of the PR were Vim^+ (**h**). **i** Immunoreactivity for GFAP in adults remains intense and restricted to Müller glia endfeet. **j** Pax2 immunofluorescence in the CR at E38. Note that the staining is restricted to nuclei residing in the middle of the INL (delimited by *vertical bar*) and in the RONJ (*arrowheads*). **k** Electron micrograph of Müller glia endfeet at E37 showing gliofilaments (*gf*) and dense bodies (*arrowheads*). Note the incipient basal lamina (*arrow*) and the immature axons of small calibre (*ax*). **l** Electron micrograph of Müller glia endfeet at E39 showing abundant cisternae of smooth (*asterisk*) and rough (*arrowheads*) endoplasmic reticulum. Note unmyelinated axons (*ax*). **m–o** Electron micrographs of Müller cells (*Mü*) in the adult retina. Note the higher electron-dense cytoplasm within the cell body compared with embryonic stages. **m** Müller cell bodies residing in the inner nuclear layer are surrounded by neuronal processes (*np*). **n** Müller glia processes in the ganglion cell layer surround and isolate retinal ganglion cells (*RGC*). **o** Note Müller glia endfeet at the peripheral retina in close contact with loose myelin in the nerve fibre layer (*arrows*). *Bars* 5 μm (**a–c**), 25 μm (**d–j**), 1 μm (**k–o**)

Characterisation of astroglial cells during ontogeny of optic nerve

By E30, abundant $Pax2^+$ nuclei were observed along the primitive ON (Fig. 3a) and a subpopulation of these nuclei clearly demarcated the RONJ until the adult stage (arrowheads in Fig. 3b, d). Ultrastructurally, this region consisted of two to three layers of elongated astroglial cells with euchromatic nuclei and scarce gliofilaments, which constituted a putative barrier between the retina and the ONH (Fig. 3c, g). In the entire ON, rows of $Pax2^+$ astroglial cells coexpressed Vim from E35 onwards (Fig. 3d) and GFAP from E37 onwards (Fig. 3e). This indicated the predominant expression of Pax2 in Vim^+ and $GFAP^+$ astroglial cells. Astrocytes in the RONJ and conus papillaris-optic nerve junction (CPONJ) were intensely Vim^+ and $GFAP^+$ (Fig. 3d–f). Accordingly, the ultrastructure of immature astrocytes in these regions showed a gradual increase of gliofilaments during development (Fig. 3g); in the adult, this was maximal in the fibrous astrocytes of the CPONJ (Fig. 3h). Astrocytes of the adult RONJ showed nuclei with clumps of heterochromatin and abundant overlapping processes, termed lamellar stacks (Fig. 3i). In the entire ON, GFAP staining became apparently stronger in late embryos and the presence of Vim^+, $GFAP^+$ and $Pax2^+$ astrocytes persisted until the adult stage (see below).

As described in the retina, $PCNA^+$ cells in the ON were more abundant in the early and medium embryonic stages (Fig. 3j), whereas they were undetectable in postnatal and adult stages (not shown). By E39, $PCNA^+$ cells were identified as subpopulations of $GFAP^+$ astrocytes (Fig. 3k, l), white blood cells (Fig. 3k) and putative $Pax2^+$ astroglia (Fig. 3m).

Ultrastructurally, differentiating astrocytes and their processes in the inner ONH and mid optic nerve (MN) showed abundant gliofilaments, microtubules, dense bodies and intercellular desmosomes (Fig. 4a, b). Putative growth cones were frequently apposed to these astrocytes (Fig. 4a).

Heterogeneous astroglial cells along ON

Remarkably, in the developing and adult ONH/MN, Vim^+ and $GFAP^+$ astroglia displayed processes oriented perpendicularly to nerve fibres (Figs. 3d–f, k, l, 4c, d). In contrast, astroglial cells in the caudal optic nerve (CN) were star-shaped (Fig. 4d). Astrocytes coexpressing Pax2, Vim and GFAP persisted and predominated along the ON in adult animals (Fig. 4c, e, f). However, a small fraction of astrocytes seemed to contain either Vim or GFAP (Fig. 4e) and few Vim^+ cells showed $Pax2^-$ nuclei. GFAP staining showed an apparent homogeneous distribution along the entire ON, with abundant expression in the MN (Fig. 4c, see also Electronic Supplementary Material, Fig. S1d), whereas that of Vim became weak in the ONH and strong in the CN (Fig. 4d; see also Electronic Supplementary Material, Fig. S1c). Astrocytes in adult ON were ultrastructurally similar to those in embryos except for a mild increase in heterochromatin clumps in their nuclei (Fig. 4g). Glycogen granules accumulated in putative astrocyte cell processes (not shown).

Glial cells invasion and astrocytes differentiation in developing optic chiasm and optic tract

In early embryos, the crossing fascicles in the optic chiasm (OCh) and OTr lacked cell bodies (Fig. 5a). Accordingly, by E34, $Pax2^+$ nuclei were abundant in the CN but undetectable in the developing OCh (Fig. 5b) and OTr. By E35, $PCNA^+$ nuclei were abundant in the periventricular cells of the hypothalamus and CN but scarce in the OCh (Fig. 5c) and, by E37-E39, a massive invasion of proliferating glia had occurred in the OCh (Fig. 5d, e, k). Strikingly, from E38 to adults, only a few scattered $Pax2^+$ nuclei were observed in the OCh, whereas they remained undetectable in the OTr (not shown). Remarkably, from E37 to adults, the astrocytes delimiting the crossing bundles in the OCh were strongly Vim^+ (Fig. 5f, h) and $GFAP^+$ (Fig. 5g) and they usually coexpressed both gliofilaments until the adult stage (Fig. 5i).

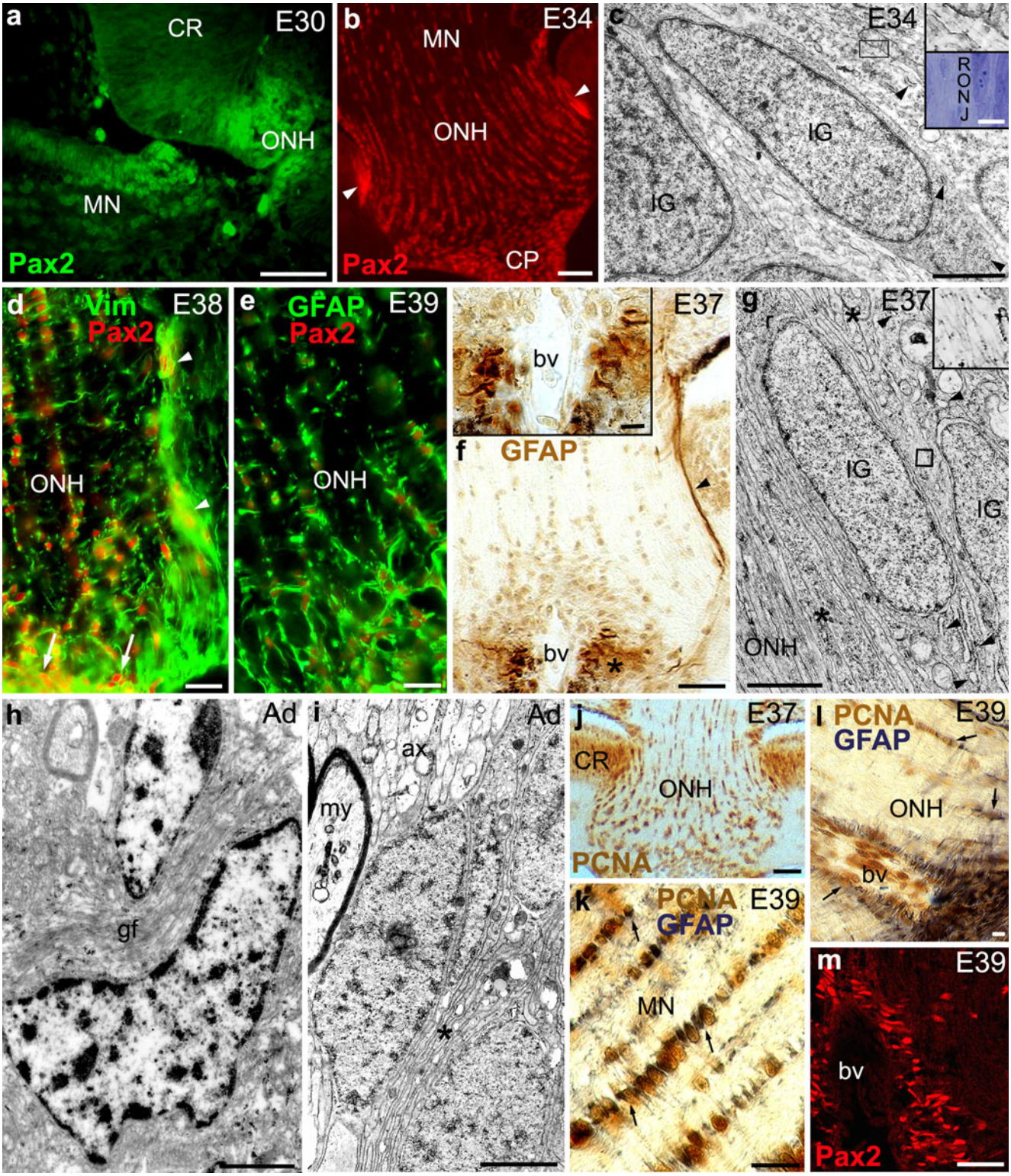

Ultrastructurally, astrocytes contained the same organelles as those of the ON.

Along similar lines, glial cells became abundant in the OTr from late embryonic stages (Fig. 5j, k). Vim staining in the developing and postnatal hypothalamus predominated in the perivascular and subpial endfeet, periventricular wall and radial glia processes (Fig. 5l). In adults, radial glia persisted in the hypothalamus being weakly Vim^{+} (Fig. 5m) and strongly $GFAP^{+}$ (Fig. 5n). Remarkably, astrocytes in the OTr expressed GFAP but not Vim (Fig. 5m, o).

Fig. 3 Pax2, Vim, PCNA and GFAP immunoreactivity and ultrastructure in the ON throughout ontogeny. **a** Pax2 immunofluorescence at E30 shows abundant staining in the primitive optic nerve head (*ONH*) and mid optic nerve (*MN*) but not in the central retina (*CR*). **b** Pax2 immunofluorescence at E34 shows intensely stained glial nuclei in the CP, ONH and MN. Note $Pax2^+$ nuclei delimiting the retina-optic nerve junction (*arrowheads*). **c** Electron micrograph of the retina-optic nerve junction (*RONJ*) at E34 corresponding to the toluidine-blue-stained semithin section shown in the *inset* (*bottom*). Elongated immature glial cells (*IG*) arranged in layers show euchromatic nuclei, short cisternae of rough endoplasmic reticulum (RER; *arrowheads*) and scarce gliofilaments (*inset*) in the medium electron-dense cytoplasm. **d** Double-staining for Vim/Pax2 at E38 reveals large colocalisation within astrocytes in the ONH, including the RONJ (*arrowheads*) and conus papillaris-optic nerve junction (CPONJ; *arrows*), which shows intense Vim staining. **e** Double-staining for GFAP/Pax2 at E39 shows extensive colocalisation of both markers in the ONH. Note intense staining in the CPONJ (*bottom*). **f** GFAP immunoreactivity in the ONH at E37 shows strong labelling in the RONJ (*arrowhead*) and CPONJ (*asterisk*; shown in detail in *inset*). **g** Electron micrograph in the RONJ at E37 showing elongated immature glial cells (*IG*) with euchromatic nuclei and abundant gliofilaments (*inset*), RER (*arrowheads*) and free ribosomes (*r*) in the medium electron-dense cytoplasm. Note numerous overlapping processes (*asterisks*). **h** Electron micrograph of a fibrous astrocyte at the CPONJ in adults. Note the clumps of heterochromatin and abundant gliofilaments (*gf*) filling the cytoplasm. **i** Electron micrograph of the adult RONJ. Astroglia exhibit prominent nucleoli and more heterochromatin clumps than in embryos (see above). Note that abundant lamellar stacks (*asterisk*) predominate in the cytoplasm. Large myelinated axons (*my*) appear intermingled with unmyelinated axons (*ax*) at the ONH side. **j** Abundant $PCNA^+$ nuclei in the ONH and central retina (*CR*) at E37. **k**, **l** Double-staining for PCNA (*brown*)/GFAP (*dark blue*) at E39 showing moderate colocalisation within differentiating astrocytes (*arrows*) in the MN (**k**) and ONH (**l**). Note GFAP staining around the central blood vessels (*bv*) with abundant proliferating leukocytes. **m** Pax2 labelling in the CPONJ at E39 shows extensive immunoreactivity around the central blood vessels (*bv*). *Bars* 25 μm (**a**, **b**, **f**, **j**, **m**), 5 μm (*insets* in **c**, **f**, **l**), 10 μm (**d**, **e**, **k**), 1 μm (**c**, **g**–**i**)

A summary of the sequential expression of astroglial markers (Pax2, Vim, GFAP) and proliferating cells in the optic pathway is shown in Table 1.

Discussion

Müller cells are the only astroglia in lizard retina and show regional differences on Vim and Pax2 staining but homogeneous GFAP labelling

Müller glia are the only astrocytic cells residing in the avascular retina of lizard, as in chick (Won et al. 2000) and guinea pig (Stanke et al. 2010). This result agrees well with the hypothesis that the presence of retinal astrocytes and blood vessels are interdependent.

The development of the vertebrate retina is a conserved process of cell genesis in which RGCs are born first and Müller glia arrive last (for a review, see Jadhav et al. 2009). As retinal progenitor cells and Müller glia share radial morphology, the Vim^+ endfeet observed in the PR of early embryos (E33), before neuronal differentiation (unpublished results), might belong to progenitor cells, whereas those from later prenatal stages most likely correspond to Müller glia as reported in chicken (Doh et al. 2010). The coexpression of Vim and GFAP in adult Müller glia also occurs in a wide variety of vertebrates from fish to mammals (De Guevara et al. 1994; Fischer et al. 2010; Gerhardt et al. 1999; Sassoè Pognetto et al. 1992, see Table 2). Gliofilaments accumulate extensively in endfeet, as described in cat and human, whereas in chick, mouse, squirrel and rabbit, Vim staining is also dense within the cell bodies (for a review, see Jadhav et al. 2009). Moreover, in the lizard retina, Müller glia endfeet show homogeneous GFAP labelling and a $centro^{low}$-$peripheral^{high}$ intensity gradient of Vim staining in inverse relation to the decreasing retinal thickness towards the periphery where it is most exposed to mechanical forces (e.g. intraocular pressure, tension of extraocular muscles insertions). Therefore, different needs for mechanical support might occur among the vertebrate retina, with more gliofilaments providing higher neuroprotection, as is also suggested by the upregulation of Vim and GFAP after retinal insults in mammals (Lewis et al. 1995). However, the normal appearance of $GFAP^-/Vim^-$ null mice retina indicates that other components of the cytoskeleton (i.e. microtubules, nestin) might be sufficient to preserve the cell morphology under normal physiological conditions, although not after retinal insults (Lundkvist et al. 2004). The proximity of loose myelin and Müller processes in the PR and the apparent absence of glial cells in this region indicate they cooperate in myelination as suggested previously (Santos et al. 2006)

Interestingly, in *G. galloti*, Müller glia express Pax2 only in the CR, as reported in zebrafish and chick (Boije et al. 2010; Stanke et al. 2010). However, retinal astrocytes are the only astroglia expressing Pax2 in mammals. In the lizard optic pathway, Pax2 might promote the glial phenotype, as in other vertebrates (Stanke et al. 2010), and its delayed expression in the retina (E37) in comparison with that in the primitive ON (E30) matches the predominance of the neurogenesis potential in the retina of the earliest embryos.

Apparent absence of a pool of stem cells in lizard retina

Proliferating stem cells are preserved in the marginal retina and local differentiated pigmented epithelium of fish, amphibians and chickens (for a review, see Mitashov 2001), being the basis for the continuous growth of amphibian and fish eyes during their lifespan. Moreover, in adult mammals, clonable and self-renewable cells have been found among the pigmented differentiated cells in the ciliary folds. Although the present study has revealed

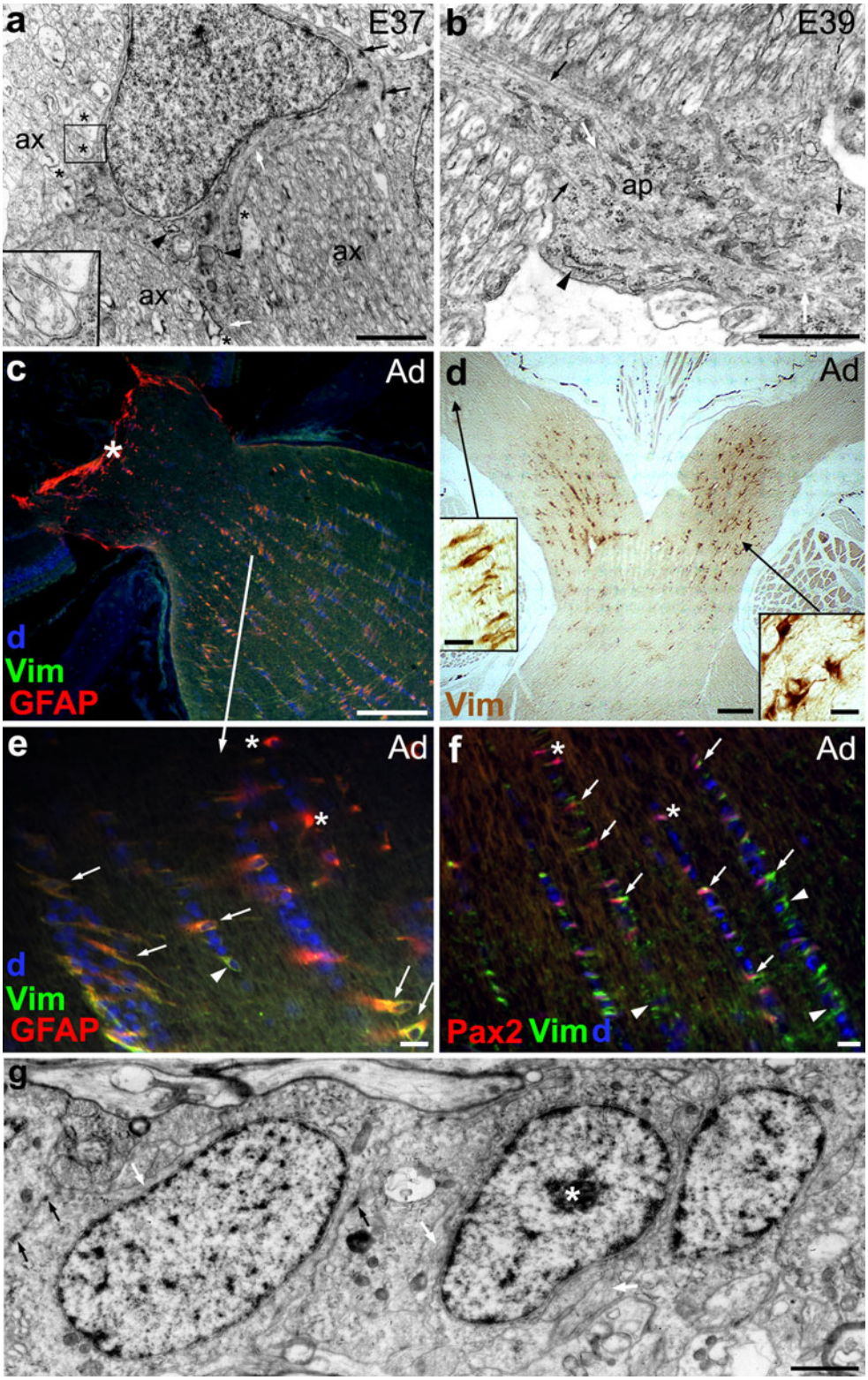

abundant proliferating cells in the developing lizard retina, they become undetectable in adults, even after ON transection (Lang et al. 2002). Thus, the adult lizard retina does not show an evident pool of proliferating stem cells. However, whether proliferation in the pigmentary epithelium has been masked by the immunoperoxidase staining or whether it persists at such a low rate to be undetectable with our methods remains to be ascertained.

◀ **Fig. 4** Vim, GFAP and Pax2 immunoreactivity and ultrastructure in the ON throughout ontogeny. **a** Star-shaped differentiating astrocytes at E37 in the MN showing desmosomes (*black arrows*), bundles of gliofilaments (*white arrows*), dilated RER (*arrowheads*), euchromatic nuclei and processes that fasciculate bundles of unmyelinated axons (*ax*). Note putative growth cones lying next to astrocytes (*asterisks*, *inset*) characterised by their thick profile containing clear vesicles. **b** Thick astroglial process (*ap*) at E39 containing dispersed microtubules (*black arrows*), short strands of dilated RER containing flocculent material (*arrowhead*) and abundant gliofilaments (*white arrows*) between axon bundles. **c** Adult lizard. Double-staining for Vim (*green*)/GFAP (*red*) and Dapi counterstaining in the ONH and MN showing the homogeneous distribution of GFAP, low Vim staining in the ONH and large colocalisation of both markers in the MN. Note strong GFAP labelling in the CPONJ (*asterisk*). **d** Vimentin staining in adult lizard. Astrocytes are more immunoreactive in the CN (*right inset*) than in the MN (*left inset*). Astrocyte processes are mainly perpendicularly oriented to the nerve fibres in the MN, whereas star-shaped astrocytes predominate in the CN. **e** Higher magnification of the MN (from **c**) showing abundant astrocytes coexpressing both types of gliofilaments (*arrows*). Cells expressing only Vim (*arrowhead*) or GFAP (*asterisks*) are sparse. $Dapi^{+}/GFAP^{-}/Vim^{-}$ cells do not belong to the astrocytic lineage. **f** Double-staining for Vim (*green*)/Pax2 (*red*) and Dapi counterstaining (*blue*) in the MN of adult animals. Note abundant $Pax2^{+}/Vim^{+}$ astrocytes (*arrows*) and some $Pax2^{-}/Vim^{+}$ (*arrowheads*) and $Pax2^{+}/Vim^{-}$ (*asterisks*) astrocytes. **g** Electron micrograph of a row of protoplasmic astrocytes in the MN of adult lizard. Gliofilaments (*white arrows*) and desmosomes (*black arrows*) are observed in the cytoplasm. Note a nucleus with clumps of heterochromatin and nucleoli (*asterisk*). *Bars* 1 μm (**a**, **b**, **g**), 100 μm (**c**, **d**), 5 μm (**e**, **f**, *insets* in **d**)

A major subset of lizard ON astrocytes sequentially express Pax2, Vim and GFAP

The sequential developmental pattern for the astroglial lineage described in the present study is reminiscent of that reported in the ON of other vertebrates. By E30, $Pax2^{+}$ cells of the primitive ON intermingle with pioneering RGC axons expressing beta-III tubulin (unpublished data) suggesting that they guide RGC axons, as reported in mouse (Alvarez-Bolado et al. 1997) and chick (Thanos et al. 2004). By E35-E37, the abundance of $PCNA^{+}$ and $Pax2^{+}$ cells in the entire lizard ON suggests that the proliferation of $Pax2^{+}$ cells is responsible for the marked increase of the astroglial population within the ON and the glial colonisation of the OCh from E35 (see below). This astrocytic proliferation might be dependent on the growth of RGCs axons, in which factors such as sonic hedgehog (Shh) are transported anterogradely mediating this proliferation in the mammalian ON (Dakubo et al. 2008).

In the central nervous system (CNS) of amniotes, Vim expression in differentiating astrocytes precedes that of GFAP. A shift to GFAP-containing intermediate filaments results in the transient coexpression of both of them and the eventual predominance of GFAP in mature astrocytes (Bodega et al. 1995; Dahl et al. 1981; Monzón-Mayor et al. 1990a). Nevertheless, most of astrocytes in the lizard ON co-expressed Vim/GFAP until adulthood, as reported in the mammalian and avian ON (Calvo et al. 1990; Fischer et al. 2010, see Table 2) and, remarkably, a few relatively mature $GFAP^{+}$ astrocytes do indeed express PCNA in late embryos. We propose that the persistent coexpression of Vim/GFAP in the ON of various vertebrates mainly reinforces the astrocyte cytoskeleton and reflects local adaptations to mechanical forces. This view is supported by the ultrastructural identification of desmosomes joining astrocytes (see below). Similarly, such coexpression occurs in brain barriers, e.g. the subpial and perivascular endfeet in the adult lizard (Monzón-Mayor et al. 1990a; Yanes et al. 1990), and in specialised astrocytes of mammals (Galou et al. 1996). Thus, mature astrocytes may coexpress Vim/GFAP in areas exposed to higher mechanical stress, although Vim has been reported as being necessary for the organisation and/or stabilisation of the GFAP intermediate filament system (Galou et al. 1996). Gliofilaments might also be involved in the cytoplasmic trafficking of exocytic vesicles (Kreft et al. 2009; Potokar et al. 2007); however, in *G. galloti*, numerous astrocytes contain secretogranin II (unpublished data) and NT-3, both in normal and axotomised ON (Santos et al. 2008), and astrocytes with vesicles containing neuropeptides and growth factors have also been detected in various vertebrate classes (Kreft et al. 2009). Thus, the astrocytic population in adult lizard ON is predominantly represented by $Pax2^{+}/Vim^{+}/GFAP^{+}$ cells, markers that are also present in the adult avian and mammalian ON, but at different levels (Stanke et al. 2010). This subpopulation differs from the $Pax2^{-}/Vim^{-}/GFAP^{+}$ astrocytes that predominate in the OTr and midbrain.

Ultrastructure reveals that lizard ON astrocytes present a delayed differentiation process and a reinforced cytoskeleton in comparison with those in midbrain

The ultrastructural features of differentiating astrocytes in the lizard ON are reminiscent of those described previously in the midbrain (Monzón-Mayor et al. 1990b) and are correlated to the immunohistochemical expression of the gliofilaments mentioned above. Thus, the numerous dark glioblasts observed around E35 in the rostral ON accumulate intermediate filaments giving rise to the abundant immature astrocytes observed by E37 and differentiate afterwards into relatively mature astrocytes with distinct clumps of heterochromatin and various contents of gliofilaments depending upon their location. Glycogen granules are mainly located in astrocyte processes in the lizard ON, allowing rapid axonal uptake of glycogen-derived lactate (Tekkök et al. 2005) supporting ON activity.

Common ultrastructural features of differentiating astrocytes in mammals and birds are microtubules and strands of dilated RER filled with flocculent material, all of which are generally

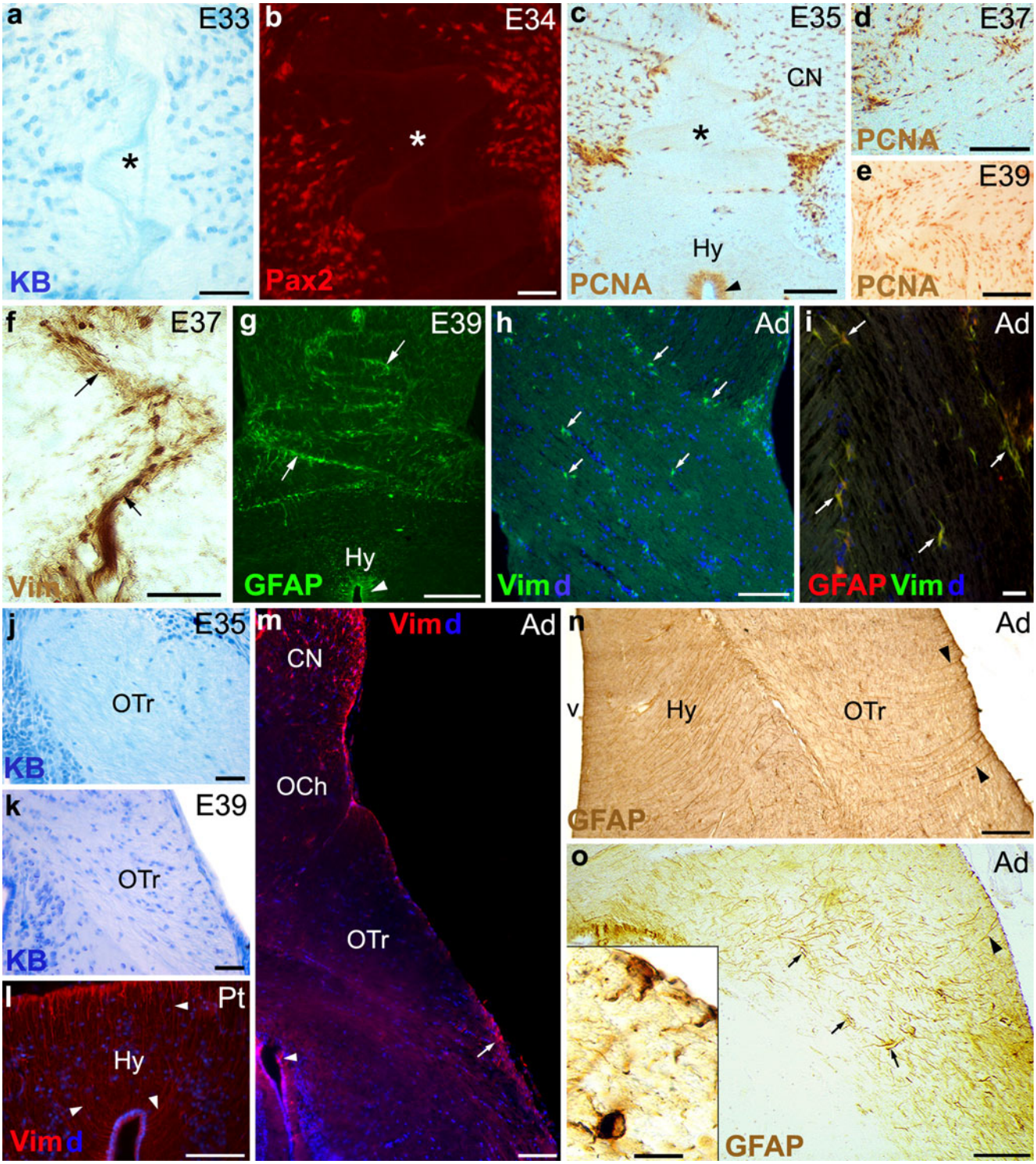

rare or undetectable in adult specimens (Fujita et al. 2001; Skoff et al. 1976; Sturrock 1975; Vaughn 1969). Interestingly, astrocytes of the lizard ON clearly show these features until the postnatal stage, whereas in the midbrain, these features are observed only until E35 (Monzón-Mayor et al. 1990b). This indicates the delayed differentiation of the astroglial lineage in the lizard ON and agrees well with the caudo-rostral gradient of maturation of the lizard CNS (Monzón-Mayor et al. 1990a; Yanes et al. 1990).

Remarkably, astrocytes show abundant intercellular desmosomes along the entire lizard ON, an observation that might be linked to Vim expression, since cytokeratin is undetectable (unpublished data). Cytokeratin^{+} astrocytes joined by desmosomes have been described in fish and

Fig. 5 Immunofluorescence and immunoperoxidase labelling for Vim, GFAP, Pax2 and PCNA during ontogeny of OCh (**a–i**) and OTr (**j–o**). **a** Klüver-Barrera staining (*KB*) in transversally cut OCh at E33. Note the lack of cell bodies in the crossing nerve fascicles (*asterisk*). **b** Pax2 labelling in transversally cut OCh at E34 reveals abundant $Pax2^+$ nuclei next to the crossing nerve fascicles, which are devoid of staining (*asterisk*). **c** PCNA staining in transversally cut OCh (*asterisk*), CN and hypothalamus (*Hy*) at E35. Note abundant proliferating cells in the CN and the hypothalamic ventricular wall (*arrowhead*), whereas only a few scattered cells are observed in the crossing nerve fascicles. **d**, **e** PCNA staining in transversally cut OCh at E37 (**d**) and E39 (**e**). Note that proliferating nuclei are more abundant at E39 than at E37. **f** At E37, Vim staining in the transversally cut OCh is intense along the borders of the decussating nerve fascicles (*arrows*). **g** Transversally cut OCh and hypothalamus (*Hy*) at E39; $GFAP^+$ astrocytes are within and at the borders of the deccusating fascicles (*arrows*). Note also $GFAP^+$ periventricular cells in the hypothalamus (*arrowhead*). **h**, **i** Horizontal sections of the adult (*Ad*) OCh. Vim^+ astrocytes persist in the crossing fascicles (*arrows* in **h**) and extensive coexpression of Vim/GFAP is detectable (*arrows* in **i**). Dapi counterstaining is shown in *blue*. **j**, **k** Klüver-Barrera staining (*KB*) in the OTr shows that the glial population is scarce at E35 (**j**) and abundant at E39 (**k**). **l** Vim^+ radial glial cells can be detected (*arrowheads*) in the postnatal (*Pt*) hypothalamus (*Hy*). **m** Horizontal section of the hypothalamus, OTr, OCh and CN of adults. Few Vim^+ periventricular cells (*arrowhead*) and subpial endfeet (*arrow*) are observed in the diencephalon. Note that Vim^+ astrocytes are stained in the CN-OCh but rarely detected in the OTr. **n**, **o** Abundant GFAP staining in the adult hypothalamus and OTr (*v* ventricle). Note immunoreactive periventricular cells and radial glial processes (*arrowheads* in **n**). Perivascular endfeet (*arrows* in **o**), subpial endfeet (*arrowhead in* **o**), astrocyte processes and cell bodies (*inset* in **o**) are extensively stained. *Bars* 25 μm (**a**, **b**, **f**, **j**, **k**) 10 μm (**i**, *inset* in **o**) 100 μm (**c–e**, **g**, **h**, **l–o**)

amphibia and are reported to represent a glial cell type that is "archaic" in evolution and "embryonic" in ontogeny, reflecting its neuroepithelial origin (Quitschke and Schechter 1986). However, true desmosomes have not been identified in glial and neuronal cells of higher vertebrates, notably mammals (Maggs and Scholes 1990; Rungger-Brändle et al. 1989). Desmosomes most likely serve to stabilise the pressure in the intraocular and extraocular ON (Jonas et al. 1991) and allow the absorption of mechanical forces linked to eye movements in cooperation with the abundant intermediate filaments. Therefore, ON astrocytes in *G. galloti* exhibit features of both low (desmosomes joining astrocytes) and high (absence of cytokeratin and presence of Vim) vertebrates, thereby supporting the intermediate phylogenetic position of such lizards.

The exclusive identification of intercellular desmosomes in the ON of regenerating vertebrates (Maggs and Scholes 1990; present study) suggests that they stabilise the astroglial scaffold, facilitating the successful regrowth of severed RGC axons. Indeed, reactive astrogliosis in the injured ON of lizard and fish is permissive for axonal regrowth (Lang et al. 2002; Levine 1993). Conversely, axonal regeneration in mammals is favoured in doubly null mutants for GFAP and Vim (Menet et al. 2003), suggesting factors other than the patterns of GFAP and Vim expression are functionally relevant for axonal regeneration in vertebrates.

Peculiar astroglia of RONJ

Glial cells at the RONJ, homologous to Kuhnt intermediate tissue in mammals, might prevent the growth of blood vessels into the developing retina, as in chick (Prada et al. 1989; Quesada et al. 2004). They express Pax2, Vim and abundant GFAP from embryonic stages, showing the same expression pattern as that reported for mammals (Chu et al. 2001); therefore, they have been classified as astrocytes. Some authors subclassify them as modified Müller cells (Hirata et al. 1991) or astroblasts (Lillo et al. 2002); however, they certainly belong to the astrocytic lineage, although they represent a peculiar glial subtype (i.e. peripapillary glia in chick). Indeed, they display different ultrastructural features and a different distribution from those of astrocytes of the CPONJ and the ONH, as reported in fish, turtle and human (Dávila et al. 1987; Lillo et al. 2002; Triviño et al. 1996). Specifically, they are elongated and packed giving rise to a special glia limitans that lacks an apparent basal lamina. Moreover, they display numerous overlapping processes that, interestingly, have also been described in lamellar stack astrocytes of the rat brain by Holen (2011) and in the fish RONJ by Lillo et al. (2002) who suggest that they allow the stretching or shrinkage of these cells as a response to local forces originating from the movement of the ocular sphere.

Morpho-functional adaptation of astrocytes along ON

Importantly, the adaptability of the astrocytes suggests that their morphological differences merely reflect variations of a single class of cell that adopts various shapes when in contact with axon bundles and/or blood vessels (Chan-Ling and Stone 1991). Astrocytes of the ONH downregulate the expression of Vim in adults, becoming restricted to its border regions, namely the RONJ and CPONJ, which also contain high levels of GFAP. Accordingly, astrocytes of the CPONJ are densely packed and clearly belong to the fibrous subtype as reported in fish, turtle and human by Dávila et al. (1987), Lillo et al. (2002) and Triviño et al. (1996); in the opinion of to these authors, the astrocytes most likely protect the RGC axons, which bend 90º in this region.

We have also observed astrocyte processes extending towards blood vessels along the ON-OTr; these might participate in the blood brain barrier like those reported in the conus papillaris (Alfayate et al. 2011). $Vim^+/GFAP^+$ astrocytes arranged in rows in the lizard MN contain more organelles in their cytoplasm, at the expense of gliofilaments, than those of the CPONJ. They display processes rich in GFAP perpendicular to RGC axons, as occurs in fish and amphibia (Maggs and Scholes 1990; Rungger-Brändle et al. 1989) suggesting that they replace the mechanical function of the absent lamina cribrosa, as in rat (Wolburg

Table 1 Qualitative changes in immunostaining for vimentin (*Vim*), glial fibrillary acidic protein (*GFAP*), transcription factor Pax2 and proliferating cell nuclear antigen (*PCNA*) during the ontogeny of the lizard visual system. Immunoreactivity (− undetected staining, ± scarce staining, + abundant staining) is indicated at the corresponding developmental stages (*E* embryonic stage). Vim, Pax2 and PCNA were expressed at least from E33. GFAP was detected from E37 and thereafter increased in intensity, being maximal in adults, whereas proliferating cells vanished in the adult lizard (*CN* caudal optic nerve, *CR* central retina, *MN* mid optic nerve, *OCh* optic chiasm, *ON* optic nerve, *ONH* optic nerve head, *OTr* optic tract, *PR* peripheral retina, *RP* radial processes)

Structure	Antigen	E33	E35	E37	E39	Adult
Retina	Vim	PR ±, CR -	PR ±, CR ±	PR +, CR ±	PR +, CR ±	PR +, CR ±
	GFAP	−	−	PR ±, CR ±	PR +, CR +	PR +, CR +
	Pax2	−	−	PR −, CR +	PR −, CR +	PR −, CR ±
	PCNA	+	+	PR +, CR ±	±	−
ON	Vim	−	±	+	+	ONH ±, MN ±, CN +
	GFAP	−	−	±	+	ONH ±, MN +, CN ±
	Pax2	+	+	+	+	+
	PCNA	+	+	+	+	−
OCh	Vim	−	−	+	+	+
	GFAP	−	−	±	+	+
	Pax2	−	±	+	+	+
	PCNA	−	±	+	+	−
		(Lack of cell bodies)				
OTr	Vim	RP +	RP +	RP +	RP ±	RP ±
	GFAP	−	−	±	+	+
	Pax2	−	−	−	−	−
	PCNA	−	−	+	+	−
		(Lack of cell bodies)				

and Bäuerle 1993), chick (Fujita et al. 2001) and turtle (Dávila et al. 1987).

In the CN, $Vim^+/GFAP^+$ astrocytes exhibit various cell arrangements and morphology, the cell rows becoming less

Table 2 Comparative expression (− undetected staining, ± weak-scarce staining, + moderate-intense staining) of Pax2 and intermediate filaments in the optic pathway of the visual system of vertebrate species (adults) representative of various classes (*CR* central retina, *ON* optic nerve, *OTr* optic tract, *RONJ* retina-optic nerve junction)

Class/species	Retina		RONJ	ON	OTr
	Müller glia	Astrocytes			
Fish (Levine 1989; Maggs and Scholes 1986, 1990; Parrilla et al. 2009; Cohen et al. 1994)		Absent		Pax2 +	Pax2 -
	Pax2 ±		Pax2 +	Cytokeratin +	Cytokeratin -
	Vim +		Vim (no data)	Vim ±	Vim + (goldfish)
	GFAP +		GFAP +	GFAP ± (goldfish ONH)	Vim - (*Cichlasoma meeki*)
				GFAP - (zebrafish)	GFAP +
Reptiles (lizard, present study)	Pax2+(CR)	Absent	Pax2 +	Pax2 +	Pax2 -
	Vim +		Vim +	Vim +	Vim ±
	GFAP +		GFAP +	GFAP +	GFAP +
Chick (Boije et al. 2010; Doh et al. 2010; Fischer et al. 2010; Kálmán et al. 1998)		Absent	*(Peripapillary glia)*		
	Pax2+(CR)		Pax2 +	Pax2 +	Pax2 (no data)
	Vim +		Vim +	Vim +	Vim -
	GFAP +		GFAP +	GFAP +	GFAP +
Rat/mouse (Calvo et al. 1990; Stanke et al. 2010)	Pax2 -	Pax2 +	Pax2 +	Pax2 +	Pax2 (no data)
	Vim +	Vim +	Vim +	Vim +	Vim (no data)
	GFAP +	GFAP +	GFAP +	GFAP +	GFAP +

evident and the astrocytes showing stellate somata with thick radially oriented processes indicative of a different reorganisation of axon bundles towards the OTr as reported in fish (Lara et al. 1998). $Vim^+/GFAP^+$ astrocytes observed along the borders of the crossing fascicles from E37 might separate fascicles and participate in axon guidance as reported in mammals (Jeffery et al. 2008) and chick (Kálmán et al. 1998). Similarly, Reese et al. (1994) have observed distinct glial domains in the OCh of ferrets, with astrocytes displaying different pools of intermediate filaments.

Delayed presence of glia in developing OCh and OTr

In the OCh of vertebrates, most of the RGC axons cross the midline and innervate the contralateral hemisphere, whereas a minor proportion of uncrossed axons from the temporal retina projects ipsilaterally (for a review, see Jeffery 2001). The percentage of the latter is higher in vertebrates with eyes located frontally. However, virtually all RGC axons decussate to the contralateral hemisphere in *G. galloti* (Lang et al. 2002) as occurs in other vertebrate species with eyes located laterally (for a review, see Jeffery 2001).

From E30 onwards, RGC axons grow along the ON among $Pax2^+$ cells, which might regulate surface molecules involved in axonal guidance as suggested in other vertebrates (for a review, see Alvarez-Bolado et al. 1997). Strikingly, cell bodies are absent in the lizard OCh-OTr between E30 and E34 indicating that most of the growing RGC axons decussate and reach the tectum with a limited glial environment as reported in other vertebrates (Jeffery 2001). Moreover, Pax2 staining is undetected in the *G. galloti* OTr as in zebrafish (Macdonald et al. 1997). However, Pax2 and its suppressing activity of Shh plays a critical role in OCh development. Pax2 null mice, like $Pax2/noi^-$ null zebrafish, are achiasmatic having totally uncrossed retinal projections and this is associated with the persistent expression of Shh in the optic recess (Macdonald et al. 1997; Torres et al. 1996). Together, these data suggest that relevant surface molecules guiding RGC axons are not only expressed by $Pax2^+$ cells. We propose that radial glial processes in the developing forebrain and midbrain are key for the guidance of the first decussating axons towards the contralateral hemisphere, like those described in the mice prechiasmatic region (Williams et al. 2003). Thus, the pioneer RGC axons might also express surface molecules to guide the later axons. Therefore, the earliest development of the *G. galloti* OCh and OTr might occur without the relevant presence of cell bodies.

From E35 onwards, the glial population in the lizard OCh increases gradually, probably because the proliferating $Pax2^+$ cells in the CN reach the OCh and stop abruptly at the limits of the OTr, as detected for $Pax2/noi^+$ astrocytes in zebrafish (Macdonald et al. 1997). Taking into account this restrictive expression of Pax2 in the vertebrate ON and its special requirement of resistance to mechanical stress, we need to ascertain whether Pax2 regulates the expression and maintenance of specific cytoskeleton proteins of desmosomes, like the cytokeratin in fish and amphibia (Rungger-Brändle et al. 1989) and probably Vim in lizards.

Concluding remarks

We conclude that Pax2, Vim and GFAP are heterogeneously expressed in Müller glia (retina) and astrocytes (ON-OCh) during lizard ontogeny. Minor subpopulations of astrocytes expressing only one of the two intermediate filaments have also been detected and, together with the $Pax2^-$ astrocytes in the OTr, reflect the high heterogeneity of this lineage. Astrocytes form a structural network reinforced with intercellular desmosomes that increase the mechanical resilience of the ON-OCh and might also facilitate the regrowth of severed RGC axons upon injury. Further characterisation of the glial environment will be relevant for wider insights into this process.

Acknowledgements The technical assistance of the Electron Microscopy Services of the University of La Laguna (ULL) and the University of Las Palmas de Gran Canaria (ULPGC) are greatly appreciated.

References

Alfayate MC, Santos E, Yanes C, Casañas N, Viñoly R, Romero-Alemán MM, Monzón-Mayor M (2011) Ontogeny of the conus papillaris of the lizard *G. galloti* and cellular response following transection of the optic nerve. Immunohistochemical and ultrastructural study. Cell Tissue Res 344:63–83

Alvarez-Bolado G, Schwarz M, Gruss P (1997) Pax-2 in the chiasm. Cell Tissue Res 290:197–200

Bixby JL, Harris WA (1991) Molecular mechanisms of axon growth and guidance. Annu Rev Cell Biol 7:117–159

Bodega G, Suarez I, Rubio M, Fernandez B (1995) Type II cytokeratin expression in adult vertebrate spinal cord. Tissue Cell 27:555–559

Boije H, Ring H, López-Gallardo M, Prada C, Hallböök F (2010) Pax2 is expressed in a subpopulation of Müller cells in the central chick retina. Dev Dyn 239:1858–1866

Brodkey JA, Gates MA, Laywell ED, Steindler DA (1993) The complex nature of interactive neuroregeneration-related molecules. Exp Neurol 123:251–270

Calvo JL, Carbonell AL, Boya J (1990) Coexpression of vimentin and glial fibrillary acidic protein in astrocytes of the adult rat optic nerve. Brain Res 532:355–357

Chan-Ling T, Stone J (1991) Factors determining the morphology and distribution of astrocytes in the cat retina: a contact-spacing model of astrocyte interaction. J Comp Neurol 303:387–399

Chu Y, Hughes S, Chan-Ling T (2001) Differentiation and migration of astrocyte precursor cells and astrocytes in human fetal retina: relevance to optic nerve coloboma. FASEB J 15:2013–2015

Cohen I, Sivron T, Lavie V, Blaugrund E, Schwartz M (1994) Vimentin immunoreactive glial cells in the fish optic nerve: implications for regeneration. Glia 10:16–29

Dahl D, Rueger DC, Bignami A, Weber K, Osborn M (1981) Vimentin, the 57 000 molecular weight protein of fibroblast filaments, is the major cytoskeletal component in immature glia. Eur J Cell Biol 24:191–196

Dakubo GD, Beug ST, Mazerolle CJ, Thurig S, Wang Y, Wallace VA (2008) Control of glial precursor cell development in the mouse optic nerve by sonic hedgehog from retinal ganglion cells. Brain Res 1228:27–42

Dávila JC, Guirado S, De La Calle A, Marín-Girón F (1987) The intra-ocular portion of the turtle *Mauremys caspica*. J Anat 151:189–198

De Guevara R, Pairault C, Pinganaud G (1994) Expression of vimentin and GFAP and development of the retina in the trout. C R Acad Sci III 317:737–741

Doh ST, Hao H, Loh SC, Patel T, Tawil HY, Chen DK, Pashkova A, Shen A, Wang H, Cai L (2010) Analysis of retinal cell development in chick embryo by immunohistochemistry and in ovo electroporation techniques. BMC Dev Biol 10:8–24

Dufaure JP, Hubert J (1961) Table de dévelopment du lizard viviparae (*Lacerta vivipara jacquin*). Arch Anat Microsc Morphol Exp 50:309–327

Dunlop SA, Tee LB, Stirling RV, Taylor AL, Runham PB, Barber AB, Kuchling G, Rodger J, Roberts JD, Harvey AR, Beazley LD (2004) Failure to restore vision after optic nerve regeneration in reptiles: interspecies variation in response to axotomy. J Comp Neurol 478:292–305

Fischer AJ, Zelinka C, Scott MA (2010) Heterogeneity of glia in the retina and optic nerve of birds and mammals. PLoS ONE 5:e10774

Fujita Y, Imagawa T, Uehara M (2001) Fine structure of the retino-optic nerve junction in the chicken. Tissue Cell 33:129–134

Galou M, Colucci-Guyon E, Ensergueix D, Ridet JL, Gimenez y Rivotta M, Privat A, Babinet C, Dupouey P (1996) Disrupted glial fibrillary acidic protein network in astrocytes from vimentin knockout mice. J Cell Biol 133:853–863

Gerhardt H, Schuck J, Wolburg H (1999) Differentiation of a unique macroglial cell type in the pecten oculi of the chicken. Glia 28:201–214

Hirata A, Kitaoka T, Isihigooka H, Ueno S (1991) Cytochemical studies of transitional area between retina and optic nerve. Acta Ophthalmol (Copenh) 69:71–75

Holen T (2011) The ultrastructure of lamellar stack astrocytes. Glia 59:1075–1083

Jadhav AP, Roesch K, Cepko CL (2009) Development and neurogenic potential of Muller glial cells in the vertebrate retina. Prog Retin Eye Res 28:249–262

Jeffery G (2001) Architecture of the optic chiasm and the mechanisms that sculpt its development. Physiol Rev 81:1393–1414

Jeffery G, Levitt JB, Cooper HM (2008) Segregated hemispheric pathways through the optic chiasm distinguish primates from rodents. Neuroscience 157:637–643

Jonas JB, Mardin CY, Schlotzer-Schrehardt U, Naumann GO (1991) Morphometry of the human lamina cribrosa surface. Invest Ophthalmol Vis Sci 32:401–405

Kálmán M, Székely AD, Csillag A (1998) Distribution of glial fibrillary acidic protein and vimentin-immunopositive elements in the developing chicken brain from hatch to adulthood. Anat Embryol (Berl) 198:213–235

Kimelberg HK (2010) Functions of mature mammalian astrocytes: a current view. Neuroscientist 16:79–106

Kreft M, Potokar M, Stenovec M, Pangrsic T, Zorec R (2009) Regulated exocytosis and vesicle trafficking in astrocytes. Ann N Y Acad Sci 1152:30–42

Lang DM, Monzón-Mayor M, Bandtlow CE, Stuermer CAO (1998) Retinal axon regeneration in the lizard *Gallotia galloti* in the presence of CNS myelin and oligodendrocytes. Glia 23:61–74

Lang DM, Romero-Alemán MM, Arbelo-Galván JF, Stuermer CA, Monzón-Mayor M (2002) Regeneration of retinal axons in the lizard *Gallotia galloti* is not linked to generation of new retinal ganglion cells. J Neurobiol 52:322–335

Lang DM, Monzón-Mayor M, Romero-Alemán MM, Yanes C, Santos E, Pesheva P (2008) Tenascin-R and axon growth-promoting molecules are up-regulated in the regenerating visual pathway of the lizard (*Gallotia galloti*). Dev Neurobiol 68:899–916

Lara JM, Velasco A, Lillo C, Jimeno D, Aijon J (1998) Characterization of the glial cells in the teleost visual pathway. In: Bernardo-Castellano (ed) Understanding glial cells. Kluwer Academic, Dordrecht, pp 3–18

Lepekhin EA, Eliasson C, Berthold CH, Berezin V, Bock E, Pekny M (2001) Intermediate filaments regulate astrocyte motility. J Neurochem 79:617–625

Levine RL (1989) Organization of astrocytes in the visual pathways of the goldfish: an immunohistochemical study. J Comp Neurol 285:231–245

Levine RL (1993) Axon dependent glial changes during optic fiber regeneration in the goldfish. J Comp Neurol 333:543–553

Lewis GP, Matsumoto B, Fisher SK (1995) Changes in the organization and expression of cytoskeletal proteins during retinal degeneration induced by retinal detachment. Invest Ophthalmol Vis Sci 36:2404–2416

Lillo C, Velasco A, Jimeno D, Cid E, Lara JM, Aijon J (2002) The glial design of a teleost optic nerve head supporting continuous growth. J Histochem Cytochem 50:1289–1302

Lundkvist A, Reichenbach A, Betsholtz C, Carmeliet P, Wolburg H, Pekny M (2004) Under stress, the absence of intermediate filaments from Muller cells in the retina has structural and functional consequences. J Cell Sci 117:3481–3488

Macdonald R, Scholes J, Strähle U, Brennan C, Holder N, Brand M, Wilson SW (1997) The Pax protein Noi is required for commissural axon pathway formation in the rostral forebrain. Development 124:2397–2408

Maggs A, Scholes J (1986) Glial domains and nerve fiber patterns in the fish retinotectal pathway. J Neurosci 6:424–438

Maggs A, Scholes J (1990) Reticular astrocytes in the fish optic nerve: macroglia with epithelial characteristics form an axially repeated lacework pattern, to which nodes of Ranvier are apposed. J Neurosci 10:1600–1614

Menet V, Prieto M, Privat A, Giménez-Ribotta M (2003) Axonal plasticity and functional recovery after spinal cord injury in mice deficient in both glial fibrillary acidic protein and vimentin genes. Proc Natl Acad Sci USA 100:8999–9004

Miller RH, Ffrench-Constant C, Raff MC (1989a) The macroglial cells of the rat optic nerve. Annu Rev Neurosci 12:517–534

Miller RH, Fulton BP, Raff MC (1989b) A novel type of glial cell associated with nodes of Ranvier in rat optic nerve. Eur J Neurosci 1:172–180

Mitashov VI (2001) Multipotent and stem cells in the developing, definitive, and regenerating vertebrate eye. Izv Akad Nauk Ser Biol 6:717–727

Monzón-Mayor M, Yanes C, Ghandour MS, De Barry J, Gombos G (1990a) Glial fibrillary acidic protein and vimentin immunohistochemistry in the developing and adult midbrain of the lizard *Gallotia galloti*. J Comp Neurol 295:569–579

Monzón-Mayor M, Yanes C, James JG, Sturrock RR (1990b) An ultrastructural study of the development of astrocytes in the midbrain of the lizard. J Anat 170:33–41

Monzón-Mayor M, Yanes C, Tholey G, De Barry J, Gombos G (1990c) Immunohistochemical localization of glutamine synthetase in mesencephalon and telencephalon of the lizard *Gallotia galloti* during ontogeny. Glia 3:81–97

Monzón-Mayor M, Yanes-Méndez C, De Barry J, Capdevilla-Carbonell C, Renau-Piqueras J, Tholey G, Gombos G (1998) Heterogeneous immunoreactivity of glial cells in the mesencephalon of a lizard: a double labeling immunohistochemical study. J Morphol 235:109–119

Morcos Y, Chan-Ling T (2000) Concentration of astrocytic filaments at the retinal optic nerve junction is coincident with the absence of intra-retinal myelination: comparative and developmental evidence. J Neurocytol 29:665–678

Onteniente B, Kimura H, Maeda T (1983) Comparative study of the glial fibrillary acidic protein in vertebrates by PAP immunohistochemistry. J Comp Neurol 215:427–436

Oyama T, Abe H, Ushiki T (2006) The connective tissue and glial framework in the optic nerve head of the normal human eye: light and scanning electron microscopic studies. Arch Histol Cytol 69:341–356

Parrilla M, Lillo C, Herrero-Turrion MJ, Arévalo R, Lara JM, Aijón J, Velasco A (2009) Pax2 in the optic nerve of the goldfish, a model of continuous growth. Brain Res 1255:75–88

Pereira A Jr, Furlan FA (2010) Astrocytes and human cognition: modelling information integration and modulation of neuronal activity. Prog Neurobiol 92:405–420

Potokar M, Kreft M, Li L, Daniel Andersson J, Pangrsic T, Chowdhury HH, Pekny M, Zorec R (2007) Cytoskeleton and vesicle mobility in astrocytes. Traffic 8:12–20

Prada FA, Espinar A, Chmielewski CE, Dorado ME, Genis-Gálvez JM (1989) Regional adaptation of Muller cells in the chick retina. A Golgi and electron microscopical study. Histol Histopathol 4:309–315

Quesada A, Prada FA, Aguilera Y, Espinar A, Carmona A, Prada C (2004) Peripapillary glial cells in the chick retina: a special glial cell type expressing astrocyte, radial glia, neuron, and oligodendrocyte markers throughout development. Glia 46:346–355

Quitschke W, Schechter N (1986) Homology and diversity between intermediate filament proteins of neuronal and nonneuronal origin in goldfish optic nerve. J Neurochem 46:545–555

Raff MC (1989) Glial cell diversification in the rat optic nerve. Science 243:1450–1455

Ramos-Steffens A (1980) Tabla del desarrollo embrionario de la lacerta *Gallotia galloti* (período de organogénesis), y aspectos de su reproducción. Minor thesis, Facultad de Biología, Universidad de La Laguna, España

Reese BE, Maynard TM, Hocking DR (1994) Glial domains and axonal reordering in the chiasmatic region of the developing ferret. J Comp Neurol 349:303–324

Romero-Alemán MM, Monzón-Mayor M, Yanes C, Arbelo-Galván JF, Lang D, Renau-Piqueras J, Negrín-Martínez C (2003) S100 immunoreactive glial cells in the forebrain and midbrain of the lizard *Gallotia galloti* during ontogeny. J Neurobiol 57:54–66

Romero-Alemán MM, Monzón-Mayor M, Yanes C, Lang D (2004) Radial glial cells, proliferating periventricular cells, and microglia might contribute to successful structural repair in the cerebral cortex of the lizard *Gallotia galloti*. Exp Neurol 188:74–85

Romero-Alemán MM, Monzón-Mayor M, Santos E, Yanes C (2010) Expression of neuronal markers, synaptic proteins, and glutamine synthetase in the control and regenerating lizard visual system. J Comp Neurol 518:4067–4087

Rubin LL, Staddon JM (1999) The cell biology of the blood-brain barrier. Annu Rev Neurosci 22:11–28

Rungger-Brändle E, Achtstätter T, Franke WW (1989) An epithelium-type cytoskeleton in a glial cell: astrocytes of amphibian optic nerves contain cytokeratin filaments and are connected by desmosomes. J Cell Biol 109:705–716

Santos E, Yanes CM, Monzón-Mayor M, del Mar Romero-Alemán M (2006) Peculiar and typical oligodendrocytes are involved in an uneven myelination pattern during the ontogeny of the lizard visual pathway. J Neurobiol 66:1115–1124

Santos E, Monzón-Mayor M, Romero-Alemán MM, Yanes C (2008) Distribution of neurotrophin-3 during the ontogeny and regeneration of the lizard (*Gallotia galloti*) visual system. Dev Neurobiol 68:31–44

Sassoè Pognetto M, Panzanelli P, Artero C, Fasolo A, Cantino D (1992) Comparative study of glial fibrillary acidic protein (GFAP) like immunoreactivity in the retina of some representative vertebrates. Eur J Histochem 36:467–477

Scholes J (1991) The design of the optic nerve in fish. Vis Neurosci 7:129–139

Skoff R, Price DL, Stocks SA (1976) Electron microscopic autoradiographic studies of gliogenesis in rat optic nerve. II. Time of origin. J Comp Neurol 169:313–334

Stanke J, Moose HE, El-Hodiri HM, Fischer AJ (2010) Comparative study of Pax2 expression in glial cells in the retina and optic nerve of birds and mammals. J Comp Neurol 518:2316–2333

Stensaas LJ (1977) The ultrastructure of astrocytes, oligodendrocytes, and microglia in the optic nerve of urodele amphibians (*A. punctatum*, *T. pyrrhogaster*, *T. viridescens*). J Neurocytol 6:269–286

Sturrock RR (1975) A light and electron microscopic study of proliferation and maduration of fibrous astrocytes in the optic nerve of human embryo. J Anat 119:223–234

Suárez I, Raff MC (1989) Subpial and perivascular astrocytes associated with nodes of Ranvier in the rat optic nerve. J Neurocytol 18:577–582

Tekkök SB, Brown AM, Westenbroek R, Pellerin L, Ransom BR (2005) Transfer of glycogen-derived lactate from astrocytes to axons via specific monocarboxylate transporters supports mouse optic nerve activity. J Neurosci Res 81:644–652

Thanos S, Püttmann S, Naskar R, Rose K, Langkamp-Flock M, Paulus W (2004) Potential role of Pax-2 in retinal axon navigation through the chick optic nerve stalk and optic chiasm. J Neurobiol 59:8–23

Torres M, Gómez-Pardo E, Gruss P (1996) Pax2 contributes to inner ear patterning and optic nerve trajectory. Development 22:3381–3391

Triviño A, Ramírez JM, Salazar JJ, Ramírez AI, García-Sánchez J (1996) Immunohistochemical study of human optic nerve head astroglia. Vision Res 36:2015–2028

Vaughn JE (1969) An electron microscopic analysis of gliogenesis in rat optic nerve. Z Zell Mikrosk Anat 94:293–327

Williams SE, Mann F, Erskine L, Sakurai T, Wei S, Rossi DJ, Gale NW, Holt CE, Mason CA, Henkemeyer M (2003) Ephrin-B2 and EphB1 mediate retinal axon divergence at the optic chiasm. Neuron 39:919–935

Wolburg H, Bäuerle C (1993) Astrocytes in the lamina cribrosa of the rat optic nerve: are their morphological peculiarities involved in an altered blood-brain barrier? J Hirnforsch 34:445–459

Won MH, Kang TC, Cho SS (2000) Glial cells in the bird retina: immunochemical detection. Microsc Res Tech 50:151–160

Yanes C, Monzón-Mayor M, Ghandour MS, De Barry J, Gombos G (1990) Radial glia and astrocytes in developing and adult telencephalon of the lizard *Gallotia galloti* as revealed by immunohistochemistry with anti-GFAP and anti-Vimentin antibodies. J Comp Neurol 295:559–568

Ye H, Hernández MR (1995) Heterogeneity of astrocytes in human optic nerve head. J Comp Neurol 362:441–452